

Article

# Heatwave Trends and the Population Exposure Over China in the 21st Century as Well as Under 1.5 °C and 2.0 °C Global Warmer Future Scenarios

Zhansheng Li <sup>1</sup>, Xiaolin Guo <sup>1</sup>, Yuan Yang <sup>1</sup> , Yang Hong <sup>1,2,\*</sup>, Zhongjing Wang <sup>1,\*</sup> and Liangzhi You <sup>3</sup>

<sup>1</sup> State Key Laboratory of Hydrosience and Engineering, Department of Hydraulic Engineering, Tsinghua University, Beijing 100084, China; lizhsh1985@yahoo.com (Z.L.); guoxl15@mails.tsinghua.edu.cn (X.G.); yangyuan15@mails.tsinghua.edu.cn (Y.Y.)

<sup>2</sup> Institute of Remote Sensing and GIS, Peking University, Beijing 100871, China

<sup>3</sup> Environment and Production Technology Division (EPTD), International Food Policy Research Institute (IFPR), Washington, DC 20006, USA; L.YOU@CGIAR.ORG

\* Correspondence: hongyang@tsinghua.edu.cn (Y.H.); zj.wang@tsinghua.edu.cn (Z.W.)

Received: 6 May 2019; Accepted: 14 June 2019; Published: 15 June 2019



**Abstract:** Heatwaves exert negative socio-economic impacts and particularly have serious effects on public health. Based on the multi-model ensemble (MME) results of 10 downscaled high-resolution Fifth Phase of the Coupled Model Intercomparison Project (CMIP5) model output from NASA Earth Exchange Global Daily Downscaled Projections (NASA-GDDP), the intensity (largest lasting time), frequency and total duration of heatwaves over China as well as population exposure in the 21st century and at 1.5 °C and 2.0 °C above pre-industrial levels are investigated by using the three indices, the Heat Wave Duration Index (HWDI), annual total frequency of heatwaves (N\_HW) and annual total days of heatwaves (T\_HW) under RCP4.5 and RCP8.5. The MME results illustrate that heatwaves are projected to become more frequent (0.40/decade and 1.26/decade for N\_HW), longer-lasting (3.78 days/decade and 14.59 days/decade for T\_HW) as well as more extreme (1.07 days/decade and 2.90 days/decade for HWDI under RCP4.5 and RCP8.5 respectively) over China. High latitude and high altitude regions, e.g., the Tibetan Plateau and northern China, are projected to experience a larger increase of intensity, frequency and the total time of heatwaves compared with southern China (except Central China). The total population affected by heatwaves is projected to increase significantly and will reach 1.18 billion in later part of the 21st century, and there will be more and more people expected to suffer long heatwave time (T\_HW) in the 21st century. Compared with a 2.0 °C global warming climate, holding the global warming below 1.5 °C can avoid 26.9% and 29.1% of the increase of HWDI, 34.7% and 39.64% for N\_TW and 35.3%–40.10% of T\_HW under RCP4.5 and RCP8.5 respectively. The half-degree less of warming will not only decrease the population exposure by 53–83 million but also avoid the threat caused by longer heatwave exposure under the two scenarios. Based on the comprehensive assessment of heatwave under the two RCP scenarios, this work would help to enhance the understanding of climate change and consequent risk in China and thus could provide useful information for making climate adaptation policies.

**Keywords:** heatwave; China; HWDI; NEX-GDDP; population exposure; 1.5 °C and 2.0 °C warmer climate

## 1. Introduction

Under global warming, climate extremes will increase in both frequency and intensity, and even more significantly than the mean climate [1]. The earth ecology, global economy, and public health are

also becoming increasingly vulnerable to these extreme events, particularly temperature extremes [2]. China has experienced an average annual temperature increase of 1.2 °C since 1960 [3]. Also, more temperature extremes have been observed recently [4,5]. For example, the summer in 2013 over eastern China, the hottest summer on record, characterized by a severe heatwave and droughts, resulted in enormous economic losses and affected more than half a billion people in China [6,7].

As typical temperature extreme events, heatwaves have severe and wide-reaching impacts on the world, such as increased wildfires, infrastructure faults, loss of livestock and crop failures, along with reduced workplace productivity and vegetation gross primary productivity (GPP). In particular, heatwaves may cause more severe impacts on public health and induce a relatively higher level of vulnerability in populations that live in urban areas.

The Paris Agreement in December 2015 set a goal to hold global warming to well below 2 °C and pursues efforts to limit it to 1.5 °C above pre-industrial levels [8]. A special report was also published in 2018 from the Intergovernmental Panel on Climate Change (IPCC) for the comparison between global warming of 1.5 °C and 2 °C above pre-industrial levels, which provides a general point that “keeping global warming below 1.5 °C rather than 2.0 °C will reduce the difficulty in adaptation and the world will suffer fewer negative impacts on intensity and frequency of extreme events” [9]. However, the global 1.5 °C and 2.0 °C warming target is just an emblematic indicator globally, and the vulnerability to global warming may vary from region to region and exhibit notable spatial heterogeneity [3]. China is very sensitive and vulnerable to climate change considering its huge population and geographic location [10–12]. Therefore, efforts for the projection of heatwave over China in the 21st century and the differentiation of risks between 1.5 °C and 2 °C global warming levels is very important for understanding global warming and also useful for elaborating any national climate mitigation policies [6].

The change trend for heatwaves under a warming climate scenario has received much attention in recent years both globally and in China [13–17]. In addition, there are also some works devoted to the investigation of the changes of heatwave and exposure at the 1.5 °C and 2 °C warming levels [8,18–22]. Over China, there has been a general significant enhancement in heat waves frequency, intensity and the area suffering from such events has expanded remarkably since the 1990s [13,23–25]. For the heatwave projection over China in the 21st century or under different global warming targets, the previous works indicate that heatwaves are expected to become more frequent, more severe, and longer lasting in the future. In terms of the spatial pattern, although there is no conscious result due to the different heatwave definition, most of the studies show that western northwest China is projected to experience more large heatwave increase [7,14,26,27]. However, except for a few studies based on regional climate model (RCM) [28,29], most of the studies are based on the original CMIP5 simulation with relatively coarse resolution (e.g., 0.5~2°) and most of the previous works mainly use a special period such as 2070–2099 to reflect the change of heatwaves in the 21st century. Moreover, special analyses of the heatwaves and risk over China for increasing of 0.5 °C from 1.5 °C to 2.0 °C are also rare.

The coarse resolution obviously cannot account for the fine-scale heterogeneity of climate variability and describe the regional heterogeneity. The heterogeneities at scales of 10–50 km are more meaningful for decision makers who require detailed information on potential impacts on crop production, local residents, hydrology, species distribution, etc.

Motivated by the need of accurate regional climate change over China, especially the change of heatwaves, this study uses the CMIP5 datasets with a spatial resolution of 0.25 ° (~25 km × 25 km) from NASA-NEX to analyze the change of heatwave over China under Representative Concentration Pathway (RCP) 4.5 and 8.5.

In order to describe the potential impact of the heatwave in China, we also examined the population exposure in the 21st century under the 1.5 °C and 2 °C warming levels combined with the high-resolution population density map under RCP4.5 and RCP8.5 scenarios.

Our objective is to provide a high-resolution projection about the temporal-spatial change of heatwave and the corresponding potential population exposure in the 21st century as well as at 1.5 °C

and 2 °C warming scenarios. Previous works have assessed the capacity of GCM from CMIP5 in reproducing the present climatology and climate variability, and also proved that CMIP5 models could reproduce well the historical heatwaves globally and in China [26,30–34]. Therefore, in the following sections, we focus on the projected changes in the heatwaves in the future.

Through the analysis with NEX-GDDP high-resolution projections, the results provide the projection of heatwaves and possible population exposures in the future. This will not only enhance the understanding of climate change and related risk under climate change conditions, but also provide detailed spatial information to illustrate the benefits of limiting global warming to 1.5 °C rather than 2 °C.

## 2. Data and Study Area

### 2.1. CMIP5 Simulations

The NEX-GDDP project provides downscaled global climate simulation results from CMIP5 with the spatial resolution of 0.25 ° (~25 km × 25 km) [28], including 21 GCM models and two of the four greenhouse gas emissions scenarios known as RCP (RCP4.5 and RCP8.5, respectively) by using a statistical downscaling algorithm. The downscaled method used in the NEX-GDDP dataset is the Bias-Correction Spatial Disaggregation (BCSD) method, which was developed by Wood et al. [29] and has been widely used in climate change simulation [30,31]. In the BCSD, the reference global data is from Global Meteorological Forcing Dataset (GMFD) for Land Surface Modeling, which was produced by the Terrestrial Hydrology Research Group at Princeton University [32]. More details about NEX-GDDP could be found in Thrasher et al. [28].

As a new generation statistically downscaled climate dataset, NEX-GDDP has been proved to give more precious and more reliable projections compared with original CMIP5 GCM simulations [25,33,34].

According to the original spatial resolution of CMIP5, we choose ten representative models, which have relatively higher original spatial resolution and are from different countries and research groups. All of these models have been widely used in the study of climate change. The institution, country and original spatial resolution information is listed in Table 1.

**Table 1.** Information on the 10 climate models used in the present analysis.

Institution	Model	Spatial Resolution (Lon×Lat, degree)	Country
Centre National de Recherches Météorologiques/Centre Européen de Recherche et Formation Avancée en Calcul Scientifique (CNRM–CERFACS)	CNRM-CM5	1.40° × 1.40°	France
Atmosphere and Ocean Research Institute (The University of Tokyo), National Institute for Environmental Studies, and Japan Agency for Marine–Earth Science and Technology (MIROC)	MIROC5	1.40° × 1.40°	Japan
National Science Foundation, Department of Energy, National Center for Atmospheric Research	CESM-BGC	0.94° × 1.25°	USA
Commonwealth Scientific and Industrial Research Organization (CSIRO) and Bureau of Meteorology (BOM), Australia	ACCESS1.0	1.25° × 1.875°	Australia
National Center For Atmospheric Research(NCAR) Commonwealth Scientific and Industrial Research Organization in collaboration with the Queensland Climate Change Centre of Excellence(CSIRO-QCCCE), Australia	CCSM4	0.94° × 1.25°	USA
CSIRO-Mk3.6.0	CSIRO-Mk3.6.0	1.875° × 1.875°	Australia
Institute for Numerical Mathematics(INM), Russia	INM-CM4	2.0° × 1.5°	Russia
Institute Pierre-Simon Laplace (IPSL), France	IPSL-CM5A-MR	1.267° × 3.750°	France
Max Planck Institute for Meteorology(MPI-M),Germany	MPI-ESM-MR	1.875 × 1.875	Germany
Meteorological Research Institute(MRI), Japan	MRI-CGCM3	1.125 × 1.125	Japan

RCP4.5 and RCP8.5 are two radiative forcing pathways to  $4.5 \text{ W/m}^{-2}$  (equivalent to 650 ppm  $\text{CO}_2$  concentration) and  $8.5 \text{ W/m}^{-2}$  (equivalent to 1370 ppm  $\text{CO}_2$  concentration) by 2100 respectively. These two scenarios could represent the expected and most serious scenarios. Therefore, these two scenarios are widely used to analyze climate change [9,16].

Based on the ten CMIP5 models results under two scenarios (RCP4.5 and RCP8.5), the Multi-Model Ensemble (MME) results based on equal-weighted strategy are used for the following analysis in the 21st century.

## 2.2. 1.5 °C and 2.0 °C Warmer Scenarios

There are two approaches (i.e., the transient and the stabilized approach) to evaluate climate change impacts under the 1.5 °C and 2.0 °C warming levels. The stabilized approach is based on the simulation by the recent Half a Degree Additional Warming, Projections, Prognosis and Impacts project (HAPPI), which is designed to provide stabilized scenarios for the 1.5 and 2.0 °C warming worlds [18,35,36]. The transient method is based on transient climate states extracted from the CMIP5 archive to evaluate climate change impacts at specific global temperature targets. In terms of the difference between these two approaches, a recent study reported that the stabilized scenarios from HAPPI are largely consistent with the transient scenarios extracted from CMIP5 simulations in agricultural regions [37]. However, so far no clear conclusion has been reached.

In this study, we chose the transient method to evaluate climate change. In order to simulate the change of heatwave at under 1.5 °C and 2 °C global warming targets, analyses are performed using time-slice periods following the method in previous studies (Gosling et al.; Leng et al.; Schewe et al.; Li et al.) [37–40]. We specifically assessed the projected change of the heatwave as well as population exposure between 1.5 °C and 2 °C warmer future over eight climate regions in China, which can help to quantify the potential benefit of limiting warming to 1.5 °C.

According to previous studies [38,39,41], the spread range of the chosen 10 CMIP5 model threshold-crossing times of 1.5 °C and 2 °C global warming above pre-industrial levels under RCP4.5 and RCP8.5 scenarios are shown in Figure 1. The MME timing of CMIP5 models when the 20-yr averaged Global Mean Temperature (GMT) reaches 1.5 and 2.0 °C above the pre-industrial period is presented in Figure 1.

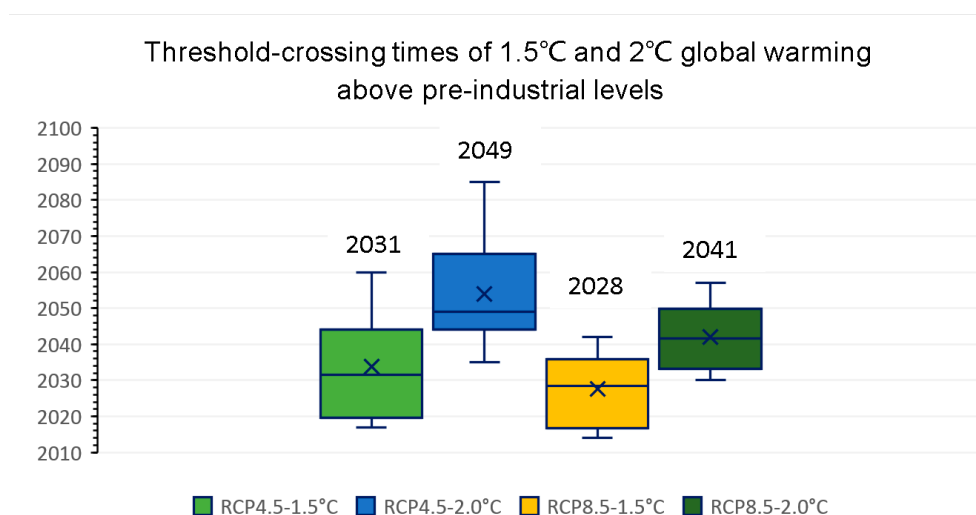


**Figure 1.** The box-plot of threshold-crossing times of 1.5 °C and 2 °C global warming above pre-industrial levels for the 10 CMIP5 models used in this study, the horizontal line within boxes and the number above the boxes represent the median result and the cross label indicates the mean result.

The global warming would exceed the 1.5 °C threshold in 2031 and 2028 under the RCP4.5 and RCP8.5 scenarios, respectively. The 2 °C global warming will occur around 2049 and 2041 under the

RCP4.5 and RCP8.5 scenarios, respectively (Figure 1). Obviously, the time to reach the two targets under RCP8.5 is shorter than that under RCP4.5. As shown in Figure 1, there is a large difference among the ten models for threshold-crossing times of 1.5 °C and 2 °C warming. For both warming targets, the spread range for the 1.5 °C and 2 °C reaching time under RCP8.5 is narrower and more consistent in comparison with those under RCP4.5.

Thus, according to Figure 1, 1.5 °C scenarios warming will be during 2021–2040 and 2018–2037 under RCP4.5 and RCP8.5, respectively, and the period of MME projection during 2041–2060 and 2030–2050 is for 2.0 °C warming scenarios. Although we just used 10 CMIP5 models, the MME threshold-crossing times of 1.5 °C and 2 °C are very close to the result based on 27 CMIP5 models [42] and the result of Li et al. by using 20 CMIP5 [43]. That means the chosen ten models have a good representation.

### 2.3. Population Density Map

In order to qualitatively analyze the population exposure of heatwaves, a China population density grid map in 2010 (1 km × 1 km) from the resource and environment data cloud platform of the Institute of Geographic Sciences and Natural Resources Research, CAS (DOI:10.12078/2017121101) was adopted. China's population density map is based on the demographic data of counties across China. It takes into account many factors such as land use type, nighttime light brightness, and residential density, which are closely related to population. Then, the population data of the administrative district is rasterized using multi-factor weight distribution method to realize the spatialization of the China population.

### 2.4. Climate Region

In order to have a better understanding of the spatiotemporal pattern of heatwave change over China on zonal perspective, China is divided into eight sub-regions (Figure 2) according to the topography and climate features following the National Assessment Report of Climate Change (2011 National Report Committee [44]).

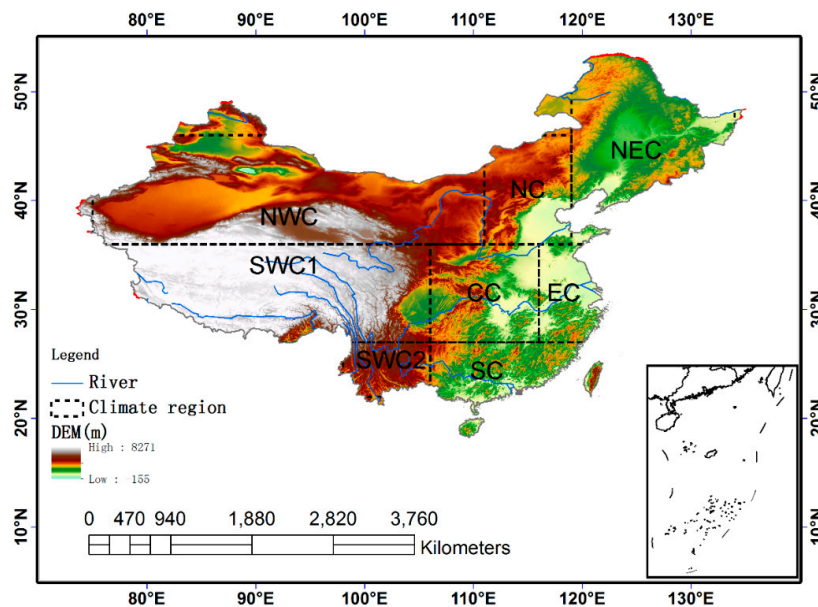


**Figure 2.** Domains of eight sub-regions in China. Northeast China (NEC): 39°N–54°N, 119°E–134°E; North China (NC): 36°N–46°N, 111°E–119°E; East China (EC): 27°N–36°N, 116°E–122°E; Central China (CC): 27°N–36°N, 106°E–116°E; South China (SC): 20°N–27°N, 106°E–120°E; Tibetan Plateau (SWC1 or TP): 27°N–36°N, 77°E–106°E; Southwest China (SWC2 or SWC): 22°N–27°N, 98°E–106°E; Northwest China (NWC): 36°N–46°N, 75°E–111°E.

### 3. Method

#### 3.1. Heatwave Indices

Heat Wave Duration Index (HWDI), which is recommended by Intergovernmental Panel on Climate Change (IPCC) [45], is used in this study to represent the severity of heatwaves. In addition, based on this index, we propose another two user-defined indexes, the annual total frequency of each heatwave (N\_HW) and annual total days of heatwaves (T\_HW) to describe the frequency and total persistent heatwave days, respectively. In order to remain in line with previous studies on climate extremes, the period 1961–1990 is adopted to be the reference period. The details of these three indices mentioned above are listed in Table 2.

**Table 2.** Definitions of three indices used in the present study.

ID	Indicator Name	Indicator Definitions	Units
HWDI	Heatwave duration index	Maximum period > 5 consecutive days with daily maximum temperature (Tamax) >5 °C above the 1961–1990 daily Tamax normal	Days
N_HW	Number of Heatwaves	The total frequency of heatwaves, which is defined as a period > 5 consecutive days with Tamax >5 °C above the 1961–1990 daily Tamax	/
T_HW	Total days of Heatwave	Annual total days for the heatwaves, which is defined as the periods > 5 consecutive days with Tamax >5 °C above the 1961–1990 daily Tamax	Days

#### 3.2. Mann-Kendall and Sen's Tests

The Mann–Kendall (MK), commonly known as Kendall's  $\tau$  statistic, is a non-parametric test used for trend analysis. The Mann-Kendall statistical test has been widely used to quantify the significance of trends in hydro-meteorological variables such as precipitation, temperature and streamflow [46–49]. The Mann-Kendall test uses a statistic value  $Z_{mk}$  to describe the trend, which is described in Mann [50,51]. Positive values of  $Z_{mk}$  indicate increasing trends while negative  $Z_{mk}$  values show decreasing trends. Testing trends are analyzed at the specific  $\alpha$  significance level. When  $|Z_{mk}| > Z_{1-\frac{\alpha}{2}}$ , the null hypothesis will be rejected and a significant trend exists in the time series.  $Z_{1-\frac{\alpha}{2}}$  is obtained from the standard normal distribution. In this study, the significance level  $\alpha = 0.05$  is used. At the 5% significance level, the null hypothesis of no trend is rejected if  $|Z_{mk}| > 1.96$ .

After the trend direction is derived by the Mann–Kendall test, the magnitude of the trend in time series data can be determined using the non-parametric method known as Sen's estimator. This method assumes a linear trend in the time series. The Sen's slope estimation is described as in Sen [52].

#### 3.3. Avoided Impacts

In order to assess the avoided impacts (AI) of heatwave under the 1.5 °C warming compared with a 2.0 °C warmer climate, a formula proposed in previous works [35,53] is used:

$$AI = \frac{C_{2.0} - C_{1.5}}{C_{2.0}} \times 100\%$$

where AI is avoided impacts,  $C_{1.5}$  and  $C_{2.0}$  are the changes for heatwave indices in 1.5 °C and 2.0 °C warming scenarios relative to 1960–1990, respectively.

## 4. Results and Discussion

### 4.1. Projected Heatwave Changes in the 21st Century

#### 4.1.1. Temporal-Spatial Heatwave Changes in the 21st Century

Figure 3 shows the change trends of HWDI, N\_HW and T\_HW under the RCP4.5 and RCP8.5 scenarios during the 21st century. Although there is a remarkable difference among the spatial patterns for the intensity, frequency and total heatwave days change rate on a decade scale, all three indices are projected to increase significantly over China under both scenarios. Overall, China is projected to experience a significant increase of HWDI (1.07 days/decade and 2.90 days/decade) and T\_HW (3.78 days/decade and 14.59 days/decade) and N\_HW (0.40/decade and 1.26/decade) in the 21st century under RCP4.5 and RCP8.5.

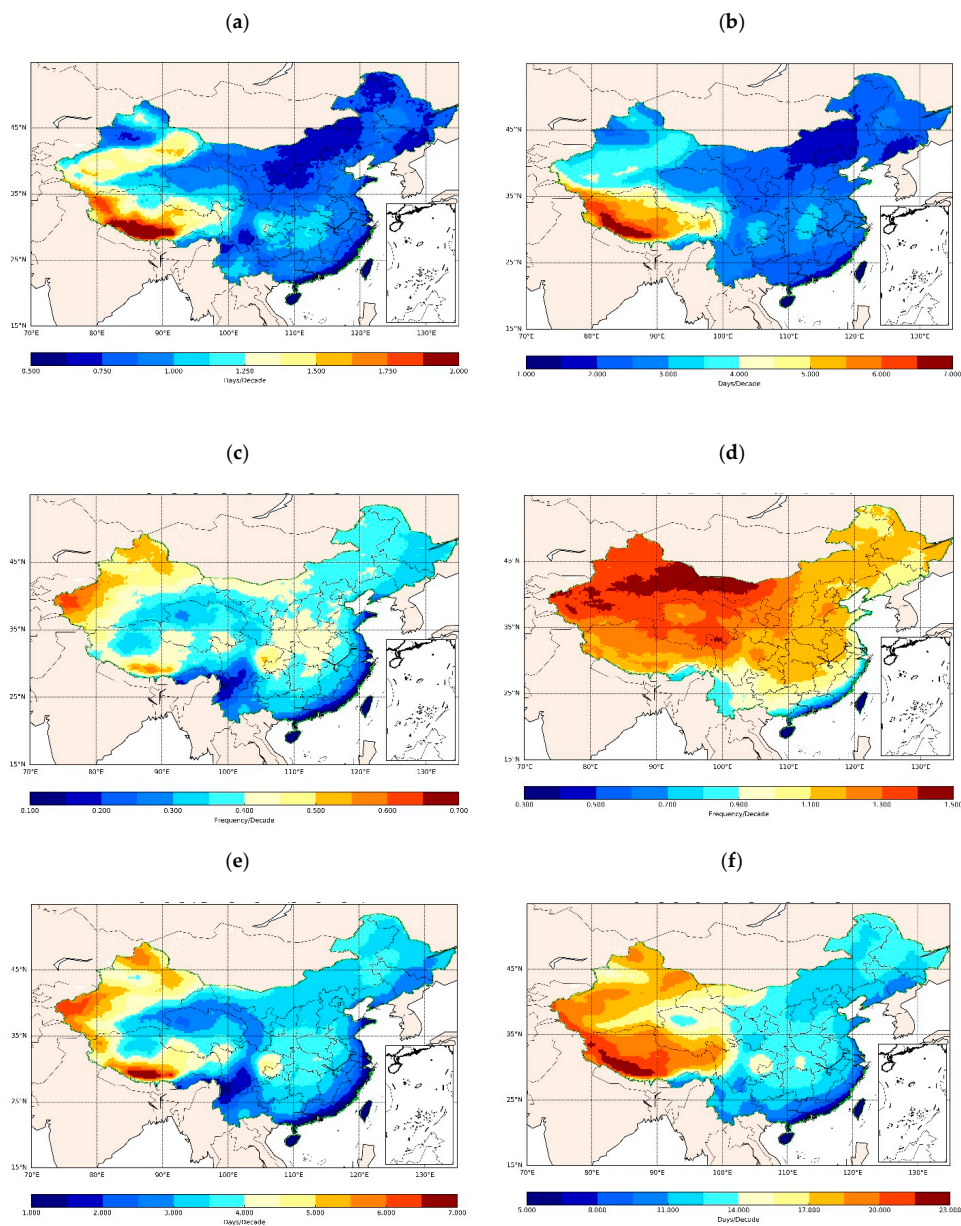


**Figure 3.** Spatial pattern of increase rate for HWDI (a,b), N\_HW (c,d), and T\_HW (e,f) during the 21st century under RCP4.5 (left: a,c,e) and RCP8.5 (right: b,d,f) by using NEX-GDDP multi-model ensemble (MME) results. The cross hatch in the image represents that there is no significant change trend at the 0.05 significance level in this pixel.

Under RCP4.5, the largest increase for HWDI will be in Northwest China and Tibetan Plateau, with more than 5 days/decade on pixel scale. Moreover, Central China also is projected to experience a larger increase for HWDI than its surrounding regions. The projection under RCP8.5 shows that the increment of HWDI is greatest in the Tibetan Plateau with a rate of 13 days/decade, closely followed by Northwest China (5 days/decade). Similar to RCP4.5, the increase rate over Central China is higher than that in neighboring regions.

Though the spatial pattern is quite similar under the two scenarios, there is a remarkable difference between the change rate of N\_HW, which under RCP8.5 is much higher than that under RCP 4.5. The increase rate for N\_HW is projected to reduce from 1.4/decade over Northwest China to 0.203/decade over South China along with the northwest-southeast direction over China under RCP8.5 (Figure 3d). Under RCP4.5, the largest increase for N\_HW will happen in Northwest China (0.46/decade), closely followed by central China (0.42/decade) and Tibetan Plateau and (0.37/decade), and the change rate in coastal regions and Southwest China (around 0.15/decade) is lowest (Figure 3c).

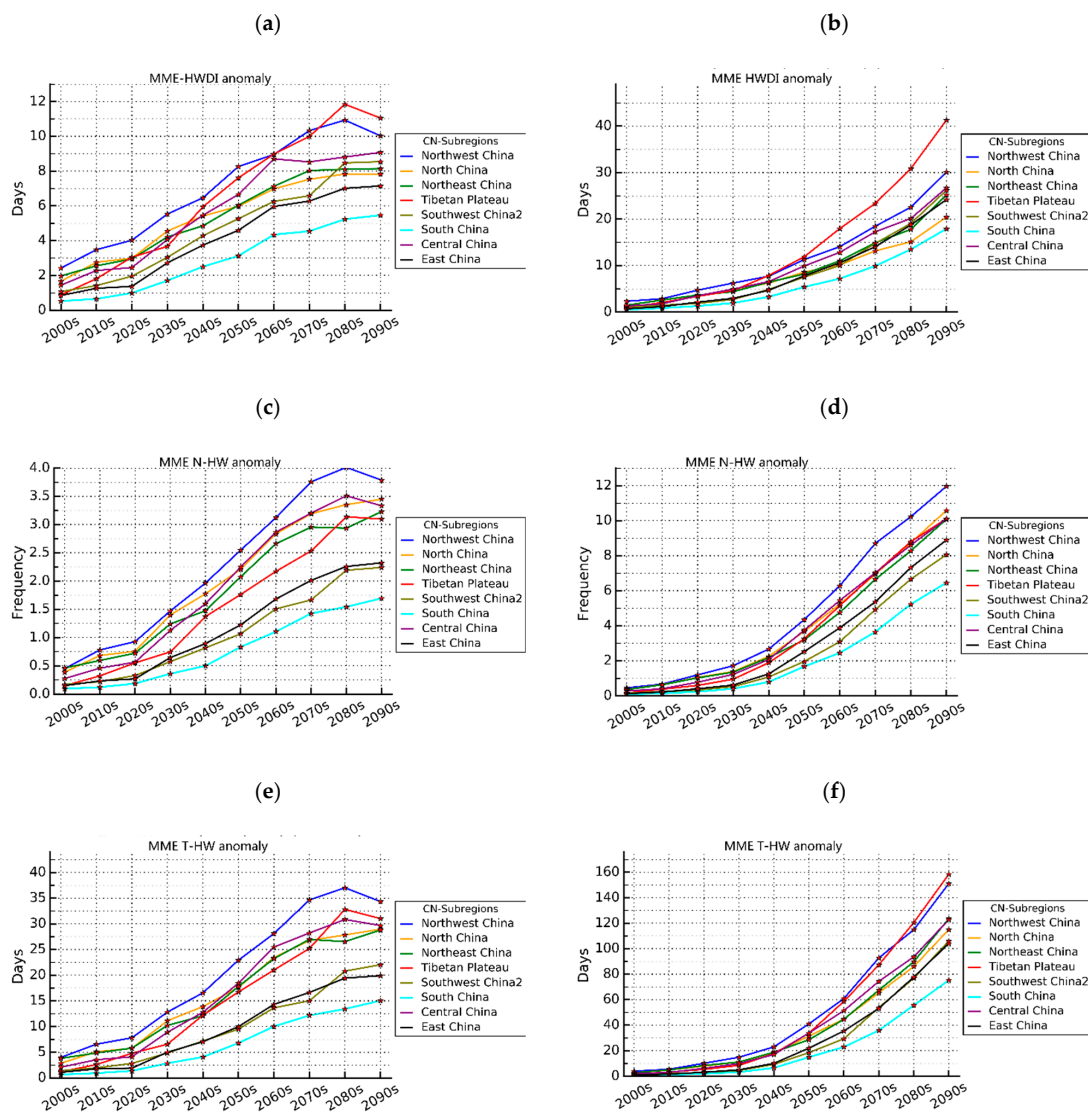
The spatial pattern of change rate for T\_HW is also similar under two scenarios. The value of T\_HW increase rate is projected to be the largest in Tibetan Plateau (3.7 days/decade and 16.7 days/decade), then next in Northwest China (4.3 days/decade and 16.3 days/decade), and Central China (3.6 days/decade and 13.6 days/decade under RCP4.5 and RCP8.5, respectively) is closely followed. In general, the increase rate for T\_HW under RCP8.5 scenario is around four times larger than that under RCP4.5 scenario, which shows the great impact of higher greenhouse emissions.

Figure 4 shows the temporal variation of HWDI, T\_HW and N\_HW over eight sub-regions relative to 1960–1991. As presented in Figure 4, the increasing trends on a regional scale for HWDI, T\_HW and N\_HW over China are more notable under both scenarios. In general, in contrast to the nearly linear increasing trend under RCP8.5, the increases of the three indices are projected to reach a peak in the 2080s under RCP4.5.

The increasing amplitude for three indices under RCP4.5 is significantly lower than that under RCP8.5. Taking N\_HW for example, the increase amplitude is in the range of 6.4–12 under RCP8.5, which is almost three times of that (1.65–3.75) under RCP4.5 in the later 21st century. The anomalies of HWDI, T\_HW and N\_HW show a similar spatial pattern, i.e., the change amplitude of these three indices over the higher altitude and latitude region is larger than that over southern China except for Central China.

As shown in Figure 4a, the largest change of HWDI is found in Northwest China and Tibetan Plateau, while South China will experience the least change of HWDI. Under RCP 8.5 (Figure 4b), the spatial characteristics are similar to those of RCP4.5. The Tibetan plateau will still experience a larger increase in HWDI in comparison with other regions under RCP8.5 than under RCP4.5.

There are some similar characteristics for HWDI and T\_HW increase pattern over the Tibetan Plateau under the two scenarios. For HWDI, the increase amplitude of Tibetan Plateau is much larger after the middle of the 21st century, and Tibetan Plateau ranks highest on the change of HWDI after the 2050s under RCP8.5. For T\_HW, under RCP4.5, the change of T\_HW in Tibetan Plateau is in middle level in comparison with other regions at the early and middle of 21st century and will rank only second to Northwest China after the 2080s, while under RCP8.5, the increase of T\_HW in the Tibetan Plateau closely follows Northwest China before the 2030s, then the increasement over this region is rather close to Northwest China and it is projected to be the region with the largest increment after the 2080s. This result implies that the increment of HWDI over the Tibetan Plateau is larger than that of T\_HW in comparison with other regions. Thus, the heatwaves will be more extreme with a higher value of HWDI. In addition, the Tibetan Plateau is more sensitive than other regions to climate warming in the middle and later of the 21st century.



**Figure 4.** Temporal variation of zonal average HWDI anomaly (a,b), N\_HW anomaly (c,d), and T\_HW (e,f) under scenario RCP4.5 (left: a,c,e) and RCP8.5 (right: b,d,f) relative to the reference period of 1961–1990 over China climate regions. The symbols on the line represent the significant linear trend of time series (star-filled red: positive trend at the 0.05 significance level; star filled blue: negative trend at the 0.05 significance level).

For N\_HW, the spatial pattern is similar under the two scenarios, with the largest increase of N\_HW occurring in Northwest China, followed by North China and Central China, and South China the least.

Regarding the projection of heatwaves, our analysis shows that China will experience more intense, more persistent and more frequent heatwaves. In general, this result is consistent with previous works [14,54,55]. In terms of spatial pattern for HWDI over Xinjiang Province, although there is a slight difference between the result presented and results from Yao et al. [14] both illustrate that the south part of the Tibetan Plateau and Xinjiang have the largest increase rate for HWDI. The spatial pattern for HWDI over southern China and eastern China is obviously different from the result in Li et al. [11]. Different from the high increase rate along the coastal area and over southwest China in Li et al., the increasing magnitude of HWDI over these regions in our work is very small in comparison with other regions. Under RCP4.5, the increase rate of HWDI is also remarkably lower than the result in Yao et al. [14] over most of China. We believe the CMIP5 model and spatial resolution are the possible reasons

for the difference between HWDI spatial patterns. In addition, among the different scenarios, our result for HWDI increase rate is significantly lower than the results under A2, A1B and B1 scenarios (9.0, 7.4 and 3.52 days/10a) [56].

Based on NEX-GDDP high-resolution projections, our results with a spatial resolution of 0.25° could present more spatial information for the HWDI change. For example, though the work of Yao et al. [14] also indicate that the south part of Tibetan Plateau and southwest of Xinjiang will experience the more increasement of HWDI over China, however, the results in Figure 3a,b clearly show that the southern part of Tibetan Plateau will experience much higher increases than Xinjiang for HWDI and the increasing rate over the northern part of Xinjiang is much lower than that over the southern part of Xinjiang Province. In addition, compared with the result with 128 × 256 Gaussian grids spatial resolution in Yao et al., the high-resolution results in this work clearly illustrate that Central China will also experience a larger HWDI increase in comparison with surrounding regions and North China will be the second-least increment region, after the coastal regions in China.

#### 4.1.2. Uncertainty of MME Heatwave Projections

Box-and-whisker plots are employed to illustrate the uncertainty of MME results and the consistency of multi-model projection among the 10 models over China’s climate regions. In general, the model spreads of HWDI, N\_HW and T\_HW under RCP8.5 are larger than that under RCP4.5 and the model spread will gradually increase in the 21st century over all the regions, especially for RCP8.5. In addition, the consistency of GCMs projections over Northeast China and South China is relatively higher than other regions under RCP4.5 and RCP8.5 (Figure 5).

(a)

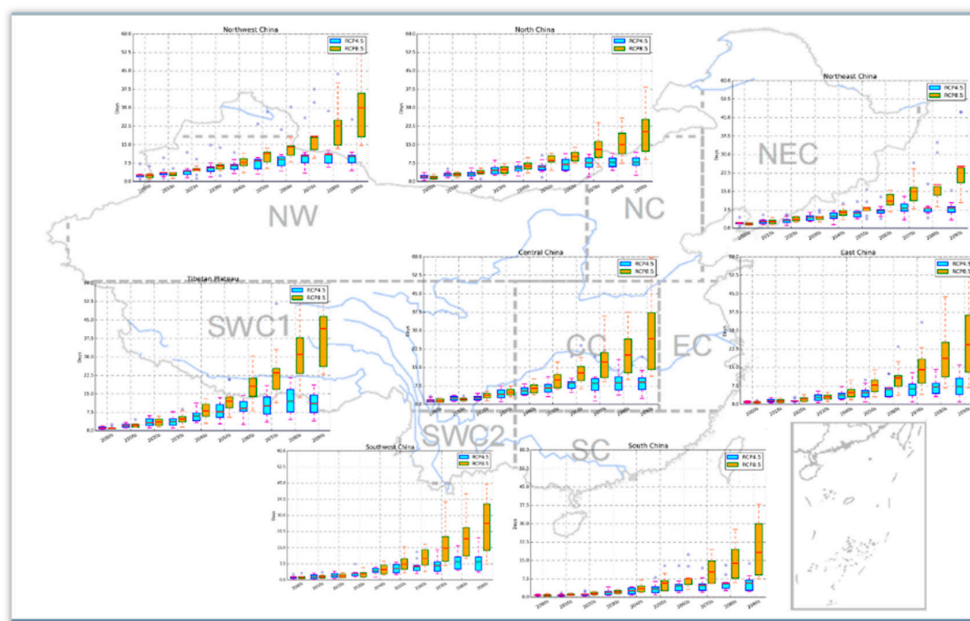
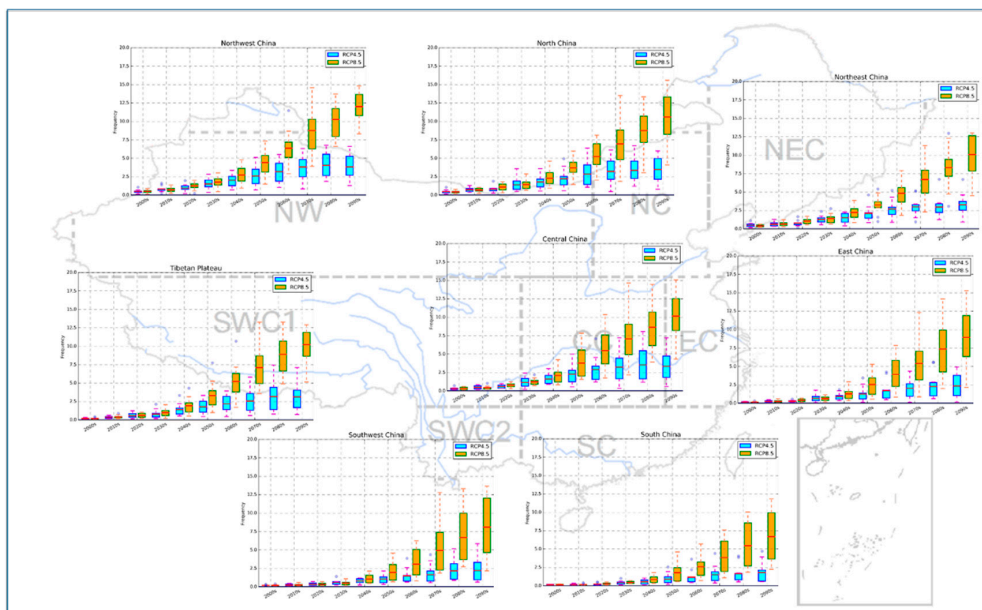
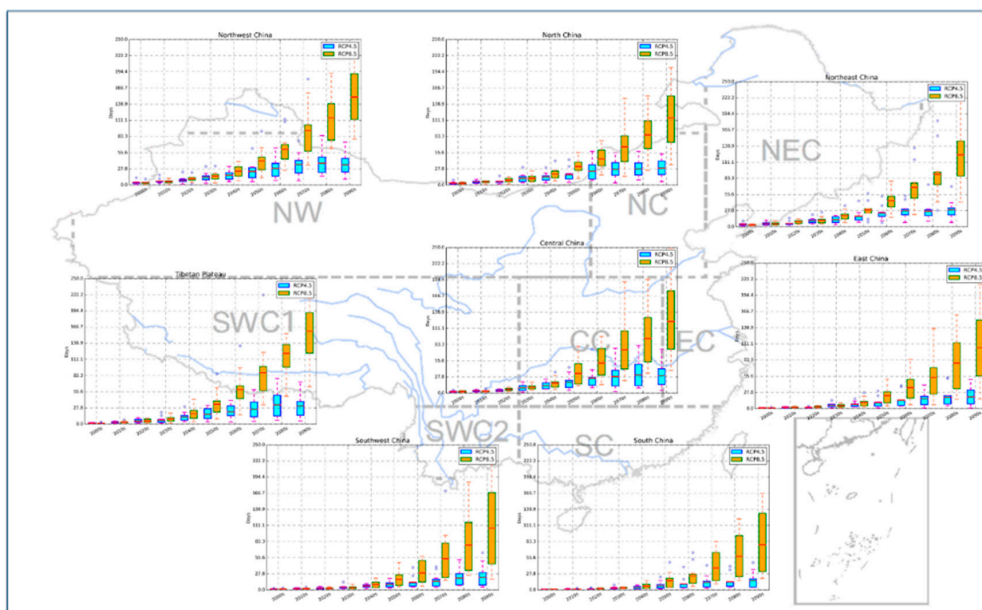


Figure 5. Cont.

(b)



(c)



**Figure 5.** Projection of HWDI (a), N\_HW (b) and T\_HW (c) anomaly over eight sub-regions during the different period in the 21st century using ten CMIP5 models under scenario RCP4.5 (cyan color) and RCP8.5 (original color) respective to 1961–1990. The central rectangle boxes indicate the interquartile spread range from the 25th to 75th quantile, the MME medians are indicated by the horizontal lines within boxes, and the extreme ranges of models are indicated by whiskers.

As shown in Figure 5, except the HWDI in the end of the 21st century under RCP8.5, all the MME projections for the three indices over different periods are located in the 25th–75th quantile of multi-model projections range, which means the MME projection is a good indicator to represent the projection of the 10 CMIP5 model results.

Note that the change of T\_HW is projected to increase by 150 days at the end of this century by some models. This result implies that heatwaves are projected to occur in any season rather than just in summer. This is caused by the definition of heatwave used in the present work.

As mentioned in the introduction, previous works have systematically assessed the capacity of GCM from CMIP5 in reproducing the present climatology and the historical changes of heatwaves over China based on ground observations [57], NCEP reanalysis dataset [14] and the  $0.5^\circ \times 0.5^\circ$  daily temperature dataset (CN05.1) over China [56,58]. In general, the CMIP5 model could reproduce the spatial pattern of HWDI and the trend in the observed period, but there is large variation for the ability of GCM in CMIP5 and over the different regions in China. On the regional scale, for example, the results in Dong et al. [58] conclude that CMIP5 tends to overestimate the HWDI over NEC, NC, SWC and underestimate the HWDI over EC in comparison with CN05.1. So far, there is no direct evaluation for the NEX-GDDP for HWDI except over Pakistan [59]. However, the ability of NEX-GDDP for daily temperature, precipitation as well as precipitation extremes over China have been evaluated over China [60,61]. The assessment provides that NEX-GDDP largely reduces the bias of temperature near-term and long-term projections in GCMs in terms of the range of absolute values as well as the spatial distribution and extremes across China [60]. Therefore, we believe that the ability of NEX-GDDP for heatwave simulation and projection have been significantly improved in comparison with the original CMIP5. Despite all this, the evolution of NEX-GDDP for HWDI is still very meaningful and needed in the future in order to understand the possible bias in heatwave-related indices projection.

#### 4.2. Population Exposure to Heatwaves in the 21st Century

As presented in Section 4.1, China is projected to experience more long, more frequent and more intense heatwaves with global warming. However, in most of China's areas, such as the sparsely populated Northwest China and Tibetan Plateau, the heatwaves would not cause a significant negative socio-economic effect, especially for public health. According to the projected spatial distribution of T\_HW on decadal, we employ China population density grid map in 2010 with a 1 km spatial resolution (DOI:10.12078/2017121101) to analyze the population exposure to heatwaves in the 21st century.

The percentage of the population affected by heatwaves (red line) is shown by the line on the right axis (Figure 6). Obviously, there is a significant increasing trend for population exposure, indicating that more and more people will be threatened by heatwaves with global warming in the 21st century. The total population affected by heatwaves is projected to reach 1.18 billion in the middle and later part of the 21st century.

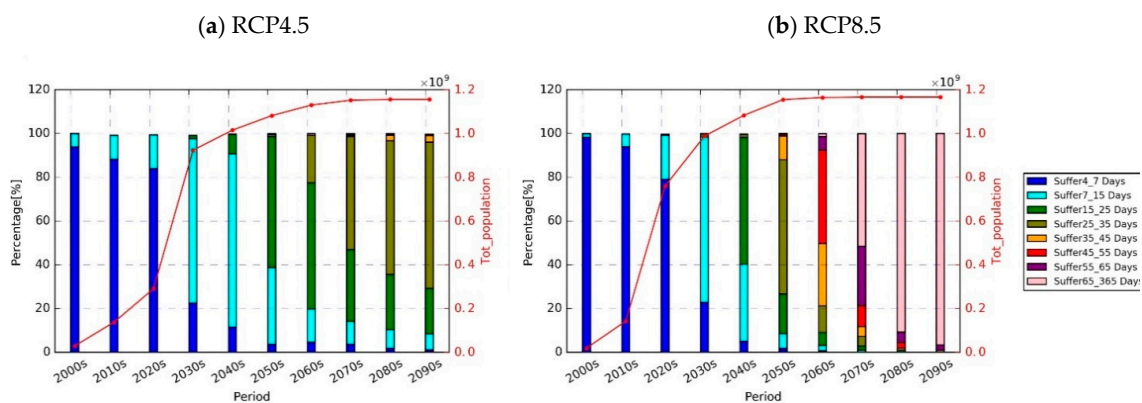


**Figure 6.** The projected temporal variation of total population (red line) threatened by the heatwave as well as the relative ratio of population influenced by different level of T\_HW (bar) in the 21st century under RCP4.5 (a) and RCP8.5 (b), with the 2010 China Population density map as the reference.

There are some differences for the population exposure temporal variation in the early part of the 21st century between the two scenarios. Under RCP4.5, there is a rapid increase for the population exposure from the 2000s to 2070s, then the population exposure will gradually increase and remain stable until the end of the 21st century, while under RCP8.5, the population exposure will increase quickly to the highest level (1.18 billion) in the 2050s.

The percentages of the population affected by different levels of heatwave days ( $T_{HW}$ ) are shown by the bar on the left axis (Figure 6). Although there is no significant difference for the total population threatened by heatwave at the later 21st century, the ratio for population exposure under longer time heatwaves, i.e.,  $T_{HW}$ , is projected to increase. At the end of the 21st century, more than 50% of 1.15 billion will be threatened by heatwaves which are longer than 25 days under RCP4.5, and the domain of heatwave persistent time will be longer than 65 days under RCP8.5. In addition, the ratio for the same level of longer  $T_{HW}$  under RCP8.5 is higher than that with RCP4.5. In other words, there will be a larger population suffering longer duration heatwaves in the future, especially under RCP4.5.

Although the population density map used in this research is based on 2010 data, the analysis could still illustrate the increase of heatwave risk and reflect the serious impact of heatwaves under global warming over China in the 21st century.

#### 4.3. Heatwave Changes Over China Under 1.5 °C and 2.0 °C Global Warming Future Scenarios

As shown in Figure 7, the region with the largest increase is projected to be Northwest China under 1.5 °C and 2.0 °C global warming scenarios and the least increase under the two warming levels will occur in the west part of Southwest China and the coastal area in southern China.

On the regional scale, the high latitude and high altitude regions are projected to suffer a larger increase of HWDI (3.9 days–5.9 days) than southern China (2.3 days–4.1 days) in 1.5 °C and 2 °C warmer futures.

In 1.5 °C warmer climate, the HWDI is projected to increase by 4.2 days and 5.8 days in Northwest China and 1.2 days and 2.0 days in the south of China under RCP4.5 and RCP8.5, respectively, while in a 2.0 °C warmer climate, it will increase by 4.9 days and 7.0 days in Northwest China and 3.0 days and 3.7 days relative to 1961–1990. In other words, the extra 0.5 °C will result in 0.7–1.2 days and 1.7–1.8 days increase in HWDI over Northwest and South China, respectively.

Note that although South China will experience the least increase for HWDI, the difference of HWDI between 1.5 °C and 2.0 °C scenarios is remarkably larger than that in Northwest China.

In order to examine the benefit of limiting global warming by 0.5 °C under RCP4.5 and RCP8.5 we use the avoided impact (AI) to investigate the heatwave indices intensity change between 1.5 °C and 2.0 °C scenarios on a regional scale. In comparison to the 2 °C warmer future, the 1.5° warming future will help avoid approximately 20%–40% of the increase of the intensity of heatwaves. The decreasing amplitude will differ over different climate regions. In addition, except in East China, Central China and Northwest China, the decreasing amplitudes are projected to be larger under RCP4.5 than RCP8.5.

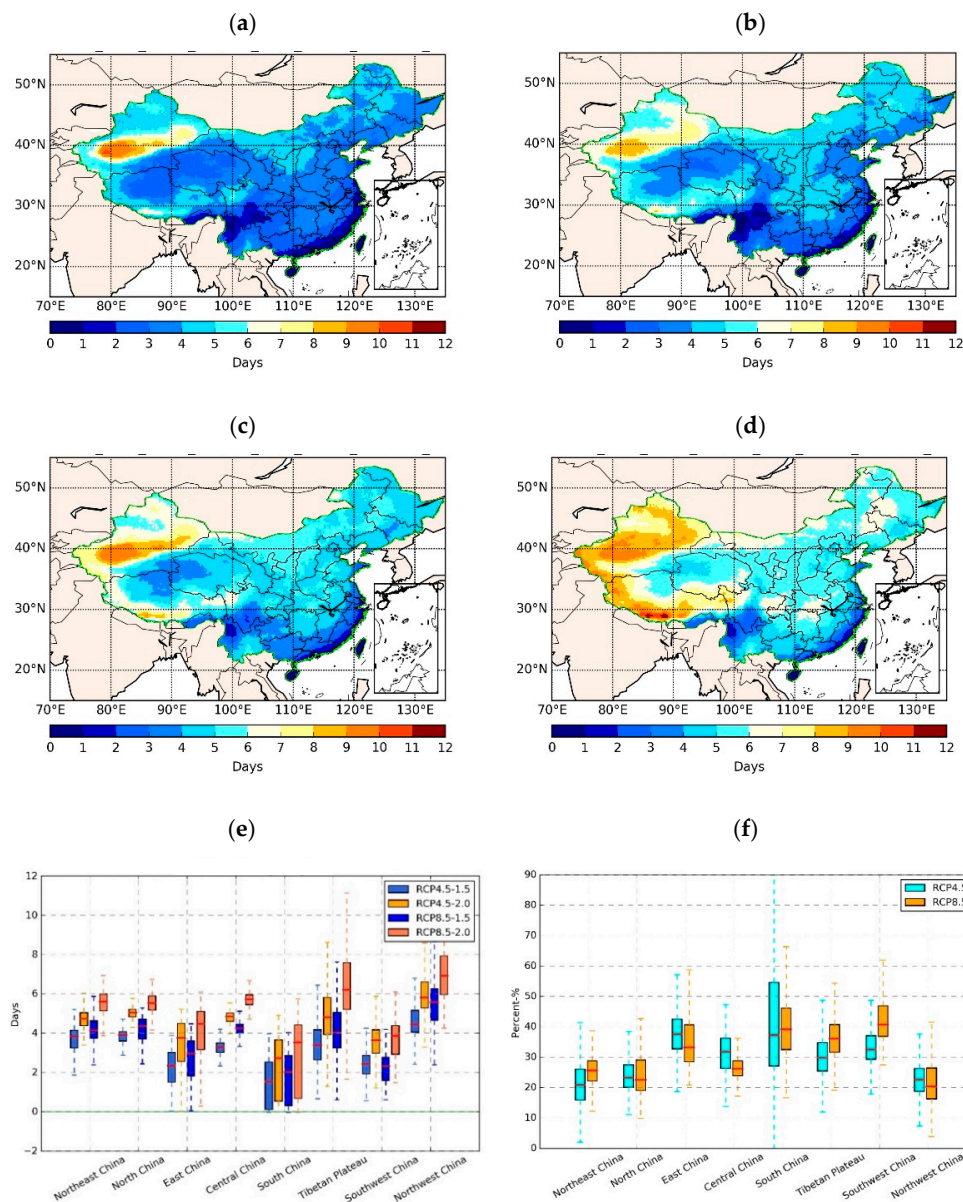


**Figure 7.** Spatial distribution of HWDI change at 1.5 °C (a,b) and 2 °C (c,d) global warming levels under scenario RCP4.5 (a,c) and RCP8.5 (b,d) relative to 1961–1990 by MME projection. Regional average of HWDI anomaly (e) and avoided impact between global warming of 1.5 °C and 2 °C above pre-industrial levels in different scenarios(f).

It should be noted that the results presented in Figure 7 about the spatial pattern of HWDI change are completely different from the results recently reported by Li et al. [53], who showed that the additional half degree of warming in the 2 °C warmer climate will result in more longer-lasting heatwave events across southern China than other regions over China. The discrepancy among the two works is partly caused by the data used. The dataset used in Li et al. is NCAR CESM low-warming simulation work, which is the stabilized projections at 1.5 °C and 2 °C warming levels. In addition, the definitions of heatwaves used in the two works are also different.

In terms of heatwave frequency, the change magnitude of N\_HW is relatively consistent between 1.5 °C and 2 °C warmer climate scenarios. Under RCP4.5 and RCP8.5, the increase of N\_HW over northern China is larger than that over southern China. Northwest China is the region with the largest increase magnitude of N\_HW (Figure 8a–d).

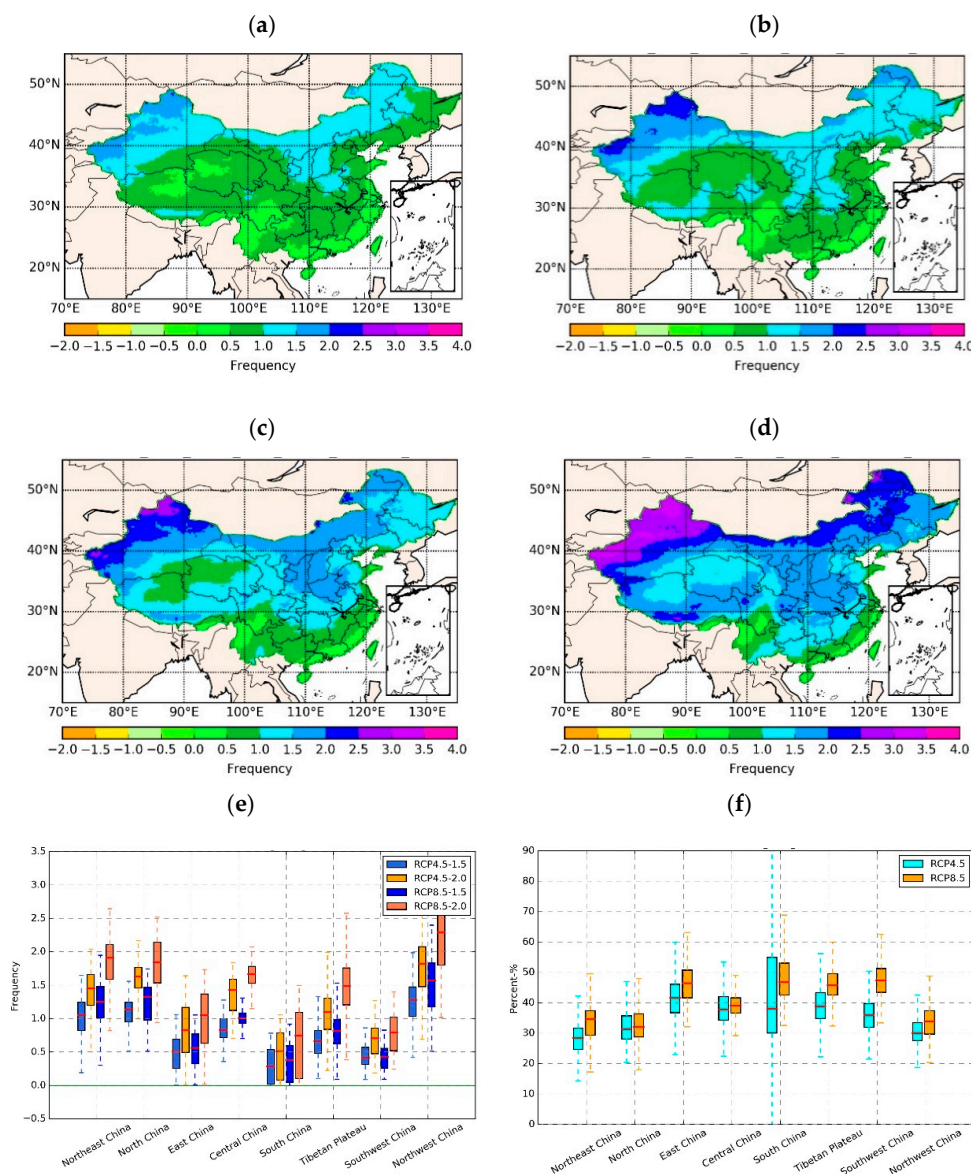


**Figure 8.** Spatial distribution of N\_HW change for 1.5 °C (a,b) and 2 °C (c,d) global warming levels under scenario RCP4.5 (a,c) and RCP8.5 (b,d) relative to 1961–1990 by MME projection. Regional average of N\_HW anomaly (e) and avoid impact between global warming of 1.5 °C and 2 °C above pre-industrial levels in different scenarios (f).

On the regional scale, the high latitude and high altitude regions are projected to experience a larger increase (1.0–1.5) than southern China (0.25–1.0) in 1.5 °C and 2 °C warmer futures as shown in Figure 8e. In addition, 1.5 °C warmer climate under RCP8.5 will avoid a larger increase magnitude of N\_HW in comparison with under RCP4.5 over eight regions. In general, limiting global warming by 0.5 °C can help avoid 28%–46% of the increases in the frequency of heatwaves over China.

In general, the spatial pattern of T\_HW is similar to that of HWDI (Figure 7a,b) and N\_HW (Figure 8a,b). T\_HW is projected to increase by 8–15 days over high latitude and high altitude regions, and by 4–8 days over southern China in 1.5 °C warmer futures. The additional half-degree warming will lead to an increase of T\_HW ranging from 12 to 19 days for high latitude and high altitude, and 7–15 days for southern China.

The change of T\_HW between 1.5 °C and 2 °C two scenarios is similar to N\_HW (Figure 9e) in terms of regional features. Under RCP4.5, holding the global warming below 1.5 °C instead of 2 °C can avoid 27%–42% of the increases in T\_HW, and it will be 32%–50% for RCP8.5.

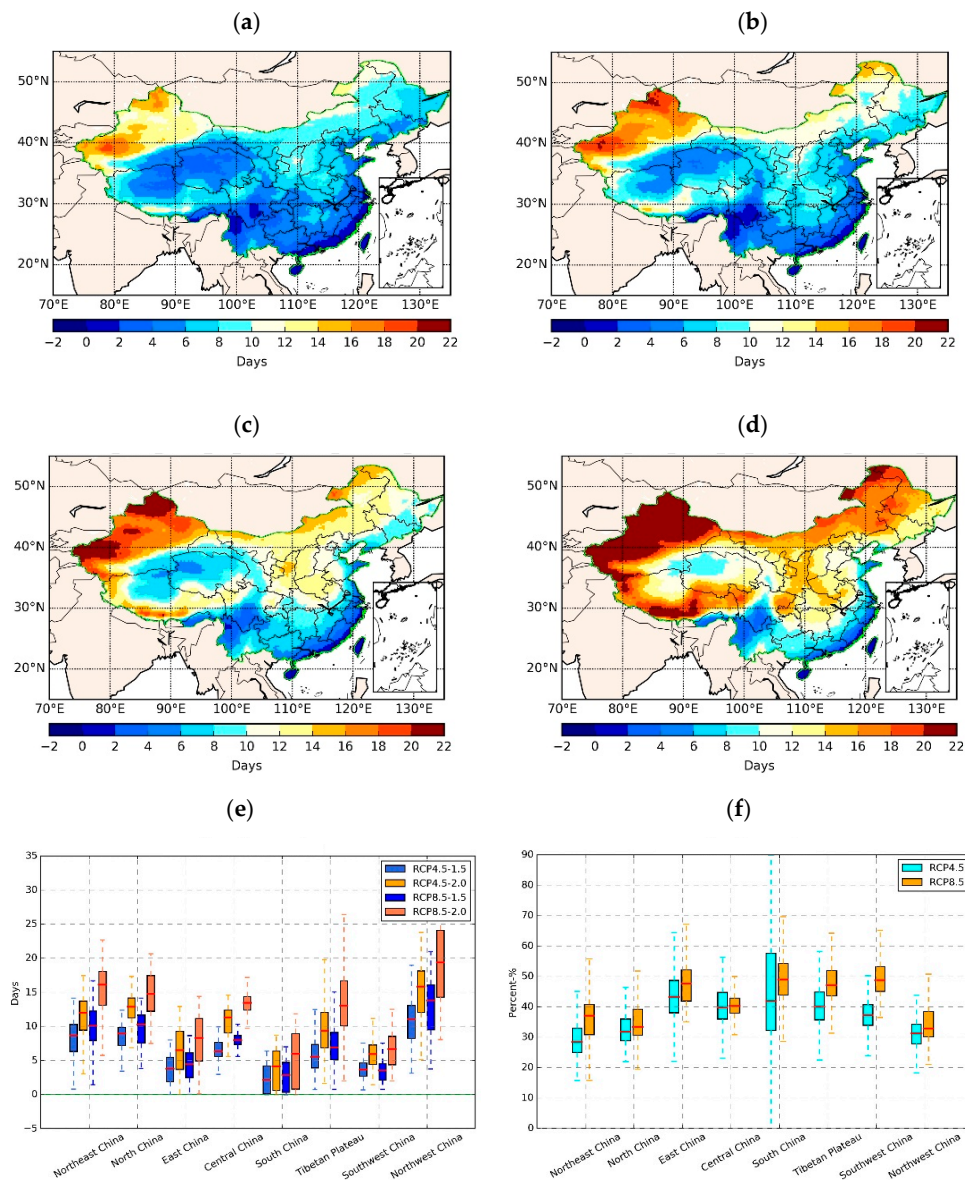


**Figure 9.** Spatial distribution of T<sub>HW</sub> change for 1.5 °C (a,b) and 2 °C (c,d) global warming levels under scenario RCP4.5 (a,c) and RCP8.5 (b,d) relative to 1961–1990 by MME projection. Regional average of T<sub>HW</sub> anomaly (e) and avoid impact between global warming of 1.5 °C and 2 °C above pre-industrial levels in different scenarios (f).

Though Guo et al. [27] also analyze the projections of heatwave characters for 1.5 °C and 2.0 °C global warmer targets, the spatial patterns of the heatwave frequency, duration and intensity are completely different from those in Figure 9. That is caused by the different heatwave definitions used in these two works.

In general, the spatial pattern of HWDI, T<sub>HW</sub> and N<sub>HW</sub> in the 21st century and in 1.5 °C and 2.0 °C warmer future scenarios show that the larger increase will be in the inland areas, especially over western China and the coastal region over China will experience the least increment. In theory, the heatwaves should increase with global warming and the spatial pattern should be consistent with that of temperature on a large scale, especially for the diurnal maximum temperature (TX). However, the heatwave is defined as prolonged periods of excessive heat (i.e., TX), which have special temporal character. This reason causes the discrepancy between the spatial pattern of heatwave change and the pattern of heatwave changes per °C warming average temperature in work of Perkins-Kirkpatrick

et al. [62] over China. In addition, the spatial pattern of heatwave trend is also similar to that of annual maximum daily maximum temperature (TX<sub>x</sub>) in Zhou et al. [26] to some degree, which implies there is a higher probability for heatwaves under higher TX on an annual scale. Thus, the spatial pattern of the heatwave change trend is between that of the maximum temperature on diurnal and annual scales.

In a word, the addition of a half-degree of warming will lead to a remarkable increase in intensity, frequency and total time for heatwaves. The increasing magnitude is higher over high latitude and high altitude regions than southern China under RCP4.5 and RCP8.5. Compared with 2.0 °C global warming, the half-degree less of warming will avoid 26.9% and 29.1% increase of HWDI, 34.7% and 39.64% for N<sub>TW</sub>, and 35.3% and 40.10% of T<sub>HW</sub> under RCP4.5 and RCP8.5, respectively.

#### 4.4. Population Exposure for 1.5 °C and 2 °C Global Warming Climate Scenarios

Similar to the results in Figure 6, the percentage of the total population affected by heatwaves (red line) is shown on the right axis (Figure 10).

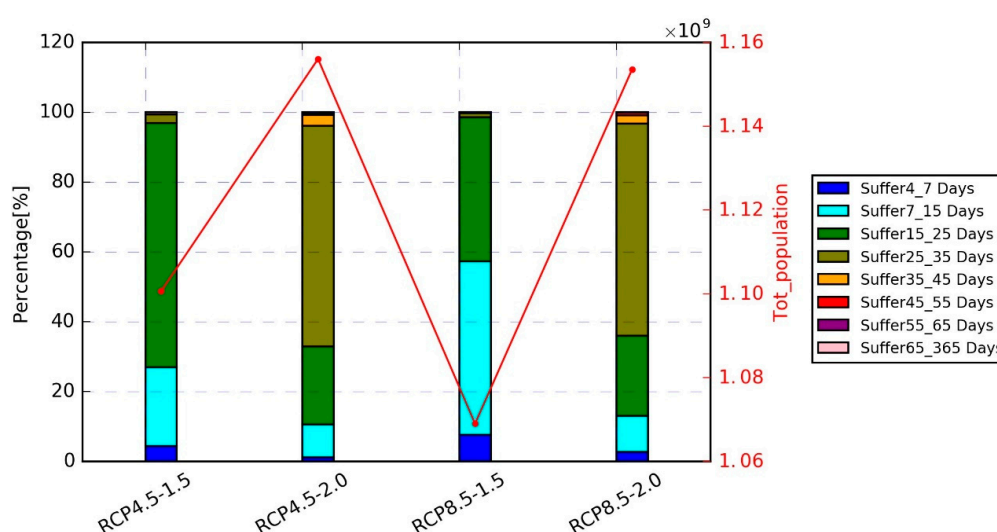


**Figure 10.** The projected total population (red line) threatened by the heatwave as well as the relative ratio of population influenced by different level of T<sub>HW</sub> (bar) by CMIP5 MME simulation for 1.5 °C and 2 °C global warming levels under scenario RCP4.5 and RCP8.5 with the 2010 China Population Density Distribution as reference.

Note that the total population exposure under RCP8.5 at 1.5 °C (1.07 billion) is lower than that under RCP4.5 (1.10 billion). However, the results illustrate that there is no notable difference between the population exposure under the two scenarios under 2.0 °C, and the total population affected by heatwaves is projected to reach 1.153 billion under 2.0 °C global warming.

Under RCP4.5, holding the global warming below 1.5 °C instead of 2 °C can avoid 83 million people from suffering heatwaves, and this number will be 53 million people under RCP8.5.

The percentages of the population threatened by different total days of heatwaves are shown through the bar on the left axis (Figure 10). The results in Figure 10 clearly illustrate that there is obviously a discrepancy between the two warming levels under the two RCP scenarios in terms of the ratio of the population suffering different heatwave durations.

At the 1.5 °C warming level, people will be mainly threatened by T<sub>HW</sub> ranging from 15 days to 25 days under RCP4.5, and the ratio of the population suffering T<sub>HW</sub> 7 days–15 days will remarkably increase under RCP8.5 in comparison with RCP4.5. Meanwhile, it should be noted that the percentage for T<sub>HW</sub> ranging from 15–25 days under RCP4.5 is much larger than that under RCP8.5 (Figure 10). Thus, China will face more heatwave risk under RCP4.5 in a 1.5 °C warmer climate compared with RCP8.5.

At 2.0 °C warming, there is no significant difference under RCP4.5 and RCP8.5 for total population exposure and the ratio for different T<sub>HW</sub>. Nearly 80% of 1.15 billion people will be threatened by T<sub>HW</sub> ranging from 15 days to 25 days and from 25 days to 35 days under RCP4.5 and RCP8.5, respectively. Therefore, holding global warming below 1.5 °C instead of 2 °C can largely avoid the threat of heatwaves longer than 25 days.

In other words, the half-degree less of warming will not only reduce the total population exposure but also significantly reduce the ratio of the population threatened by longer T<sub>HW</sub> under both RCP4.5 and RCP8.5. Thus, it will largely reduce the heatwave risk for public health.

Compared with other studies related to the population exposure to heatwaves under global warming, our results share similar trends but with different values. One main possible reason is that heatwaves can be described and categorized by various definitions and indexes (based on mean, maximum, minimum temperature, humidity, and a combination of those), which can lead to different quantitative results. For example, Zhan et al. [63] analyzed the extreme maximum temperature events (EMTES) and population exposure under global warming scenarios of 1.5 °C and 2.0 °C by using regional scale cosmo-CLM over China. Their result shows that the population exposure is projected to increase by (70.3–91.07) and (86.18–108.65) million, respectively, relative to the reference period. Compared with 2.0 °C warming, the population exposure will decrease by 0.49–25.16 million under 1.5 °C warming. Obviously, our result shows that the population exposure will be near ~80% of the China total population and 53–83 million people will avoid the threat of the heatwave in 1.5 °C in comparison with 2.0 °C warming future scenarios.

## 5. Conclusions

This paper projects the changes of the heatwave and population exposure over China during the 21st century and at 1.5 °C and 2.0 °C global warming under RCP4.5 and RCP8.5 scenarios by using Multi-Mode Ensemble (MME) results based on ten CMIP5 models with a spatial resolution of 0.25° from NASA-GDDP. The major conclusions about heatwaves can be summarized as follows:

- (1) Heatwaves are projected to become more extreme (1.07 days/decade and 2.90 days/decade for HWDI), more frequent (0.40/decade and 1.26/decade for N<sub>HW</sub>) as well as longer-lasting (3.78 days/decade and 14.59 days/decade for T<sub>HW</sub>) over China under RCP4.5 and RCP8.5, respectively, with significant spatial variation.
- (2) The spatial pattern of three heatwave indices is similar under the two scenarios while the increase will be considerably intensified under RCP8.5. From a zonal perspective, the high-resolution CMIP5 projections show that high latitude and high altitude regions, e.g., the Tibetan Plateau and northern China, are projected to experience a larger increase in intensity, frequency and the total duration of heatwaves than that in southern China (except for Central China).
- (3) According to NEX-GDDP 25 km heatwave projections, the total population affected by heatwaves is projected to significantly increase and will reach 1.18 billion in the middle and later part the 21st century based on the 2010 population density map. In addition, more and more people will suffer a longer duration of total annual heatwaves in the 21st century.
- (4) Compared with 2.0 °C global warming, holding the global warming below 1.5 °C can largely reduce the threat of the heatwaves, with HWDI decreasing by 26.9% and 29.1%, N<sub>HW</sub> decreasing by 34.7% and 39.64% as well as T<sub>HW</sub> decreasing by 35.3% and 40.10% under RCP4.5 and RCP8.5, respectively.
- (5) Population exposure will be 1.07–1.10 billion and 1.153 billion for 1.5 °C and 2.0 °C warming climates, respectively. The half-degree less of warming will not only reduce the population exposure by 83–53 million but also greatly reduce the threat caused by longer heatwave exposure under both the RCP4.5 and RCP8.5 scenarios.

With the CMIP5 MME projections at 25 km spatial resolution, this study could provide more comprehensive information about heatwaves and population exposure under two RCP scenarios in

the 21st century, especially for 1.5 °C and 2.0 °C warming cases. Compared with the rural areas, the urban areas are more sensitive and vulnerable to heatwaves. Therefore, further works should focus on the heatwave risk for the city agglomeration, which in the future will have more population and social-economic activities.

**Author Contributions:** Z.L. and Y.H. designed this Manuscript; Y.Y. provided the data; Z.L. processed the data and wrote this manuscript; X.G., Y.Y. and L.Y. modified and polished this manuscript; Y.H. and L.Y., funding acquisition; Z.W. supervision.

**Funding:** This research was funded by the National Natural Science Foundation of China, grant number. 71461010701 and 41701385.

**Acknowledgments:** This research paper was conducted at Department of Hydraulic Engineering, Tsinghua University. Thanks also to NASA for providing NEX-GDDP CMIP5 dataset.

**Conflicts of Interest:** The authors declare no conflict of interest.

## References

1. Coumou, D.; Rahmstorf, S. A decade of weather extremes. *Nat. Clim. Chang.* **2012**, *2*, 491–496. [[CrossRef](#)]
2. Kunkel, K.E.; Andsager, K.; Easterling, D.R. Long-Term Trends in Extreme Precipitation Events over the Conterminous United States and Canada. *J. Clim.* **1999**, *12*, 2515–2527. [[CrossRef](#)]
3. Piao, S.; Ciais, P.; Huang, Y.; Shen, Z.; Peng, S.; Li, J.; Zhou, L.; Liu, H.; Ma, Y.; Ding, Y.; et al. The impacts of climate change on water resources and agriculture in China. *Nature* **2010**, *467*, 43. [[CrossRef](#)] [[PubMed](#)]
4. Wang, H.-J.; Sun, J.-Q.; Chen, H.-P.; Zhu, Y.-L.; Zhang, Y.; Jiang, D.-B.; Lang, X.-M.; Fan, K.; Yu, E.-T.; Yang, S. Extreme climate in China: Facts, simulation and projection. *Meteorol. Z.* **2012**, *21*, 279–304. [[CrossRef](#)]
5. Zhai, P.; Pan, X. Trends in temperature extremes during 1951–1999 in China. *Geophys. Res. Lett.* **2003**, *30*, 169–172. [[CrossRef](#)]
6. Zhou, T.; Ma, S.; Zou, L. Understanding a hot summer in central eastern China: Summer 2013 in context of multimodel trend analysis. *Bull. Am. Meteorol. Soc.* **2014**, *95*, S54–S57.
7. Sun, Y.; Zhang, X.; Zwiers, F.W.; Song, L.; Wan, H.; Hu, T.; Yin, H.; Ren, G. Rapid increase in the risk of extreme summer heat in Eastern China. *Nat. Clim. Chang.* **2014**, *4*, 1082–1085. [[CrossRef](#)]
8. Hulme, M. 1.5 °C and climate research after the Paris Agreement. *Nat. Clim. Chang.* **2016**, *6*, 222. [[CrossRef](#)]
9. Intergovernmental Panel on Climate Change. *Global Warming of 1.5 °C: An IPCC Special Report on the Impacts of Global Warming of 1.5 °C Above Pre-Industrial Levels and Related Global Greenhouse Gas Emission Pathways, in the Context of Strengthening the Global Response to the Threat of Climate Change, Sustainable Development, and Efforts to Eradicate Poverty*; Intergovernmental Panel on Climate Change: Incheon, Korea, 2018.
10. Fang, J.; Yu, G.; Liu, L.; Hu, S.; Chapin, F.S. Climate change, human impacts, and carbon sequestration in China. *Proc. Natl. Acad. Sci. USA* **2018**, *115*, 4015–4020. [[CrossRef](#)] [[PubMed](#)]
11. Li, J.; Zhang, Q.; Chen, Y.D.; Singh, V.P. GCMs-based spatiotemporal evolution of climate extremes during the 21st century in China. *J. Geophys. Res. Atmos.* **2013**, *118*, 11017–11035. [[CrossRef](#)]
12. Huang, J.; Zhai, J.; Jiang, T.; Wang, Y.; Li, X.; Wang, R.; Xiong, M.; Su, B.; Fischer, T. Analysis of future drought characteristics in China using the regional climate model CCLM. *Clim. Dyn.* **2018**, *50*, 507–525. [[CrossRef](#)]
13. You, Q.; Jiang, Z.; Kong, L.; Wu, Z.; Bao, Y.; Kang, S.; Pepin, N. A comparison of heat wave climatologies and trends in China based on multiple definitions. *Clim. Dyn.* **2017**, *48*, 3975–3989. [[CrossRef](#)]
14. Yao, Y.; Yong, L.; Jian-Bin, H. Evaluation and projection of temperature extremes over China based on CMIP5 model. *Adv. Clim. Chang. Res.* **2012**, *3*, 179–185. [[CrossRef](#)]
15. Meehl, G.A.; Tebaldi, C. More intense, more frequent, and longer lasting heat waves in the 21st century. *Science* **2004**, *305*, 994–997. [[CrossRef](#)] [[PubMed](#)]
16. Wang, P.; Hui, P.; Xue, D.; Tang, J. Future projection of heat waves over China under global warming within the CORDEX-EA-II project. *Clim. Dyn.* **2019**. [[CrossRef](#)]
17. Im, E.-S.; Pal, J.S.; Eltahir, E.A.B. Deadly heat waves projected in the densely populated agricultural regions of South Asia. *Sci. Adv.* **2017**, *3*, e1603322. [[CrossRef](#)] [[PubMed](#)]
18. Mitchell, D.; AchutaRao, K.; Allen, M.; Bethke, I.; Beyerle, U.; Ciavarella, A.; Forster, P.M.; Fuglestedt, J.; Gillett, N.; Haustein, K. Half a degree additional warming, prognosis and projected impacts (HAPPI): Background and experimental design. *Geosci. Model Dev.* **2017**, *10*, 571–583. [[CrossRef](#)]

19. Suhaila, J.; Yusop, Z. Trend analysis and change point detection of annual and seasonal temperature series in Peninsular Malaysia. *Meteorol. Atmos. Phys.* **2018**, *130*, 565–581. [[CrossRef](#)]
20. Chevuturi, A.; Klingaman, N.P.; Turner, A.G.; Hannah, S. Projected changes in the Asian-Australian monsoon region in 1.5 °C and 2.0 °C global-warming scenarios. *Earths Future* **2018**, *6*, 339–358. [[CrossRef](#)]
21. Nikulin, G.; Lennard, C.; Dosio, A.; Kjellström, E.; Chen, Y.; Hänsler, A.; Kupiainen, M.; Laprise, R.; Mariotti, L.; Maule, C.F. The effects of 1.5 and 2 degrees of global warming on Africa in the CORDEX ensemble. *Environ. Res. Lett.* **2018**, *13*. [[CrossRef](#)]
22. Dosio, A.; Mentaschi, L.; Fischer, E.M.; Wyser, K. Extreme heat waves under 1.5 °C and 2 °C global warming. *Environ. Res. Lett.* **2018**, *13*, 054006. [[CrossRef](#)]
23. Ding, T.; Qian, W. Geographical patterns and temporal variations of regional dry and wet heatwave events in China during 1960–2008. *Adv. Atmos. Sci.* **2011**, *28*, 322–337. [[CrossRef](#)]
24. Dian-Xiu, Y.; Ji-Fu, Y.; Zheng-Hong, C.; You-Fei, Z.; Rong-Jun, W. Spatial and temporal variations of heat waves in China from 1961 to 2010. *Adv. Clim. Chang. Res.* **2014**, *5*, 66–73. [[CrossRef](#)]
25. Ding, T.; Ke, Z. Characteristics and changes of regional wet and dry heat wave events in China during 1960–2013. *Theor. Appl. Climatol.* **2015**, *122*, 651–665. [[CrossRef](#)]
26. Zhou, B.; Wen, Q.H.; Xu, Y.; Song, L.; Zhang, X. Projected Changes in Temperature and Precipitation Extremes in China by the CMIP5 Multimodel Ensembles. *J. Clim.* **2014**, *27*, 6591–6611. [[CrossRef](#)]
27. Guo, X.; Huang, J.; Luo, Y.; Zhao, Z.; Xu, Y. Projection of heat waves over China for eight different global warming targets using 12 CMIP5 models. *Theor. Appl. Climatol.* **2017**, *128*, 507–522. [[CrossRef](#)]
28. Yang, H.; Xu, Y.; Zhang, L.; Pan, J.; Li, X. Projected change in heat waves over China using the PRECIS climate model. *Clim. Res.* **2010**, *42*, 79–88. [[CrossRef](#)]
29. Wang, P.; Tang, J.; Sun, X.; Liu, J.; Juan, F. Spatiotemporal characteristics of heat waves over China in regional climate simulations within the CORDEX-EA project. *Clim. Dyn.* **2019**, *52*, 799–818. [[CrossRef](#)]
30. Ying, X.U.; Chong-Hai, X.U. Preliminary Assessment of Simulations of Climate Changes over China by CMIP5 Multi-Models. *Atmos. Ocean. Sci. Lett.* **2012**, *5*, 489–494. [[CrossRef](#)]
31. Chong-Hai, X.; Ying, X. The Projection of Temperature and Precipitation over China under RCP Scenarios using a CMIP5 Multi-Model Ensemble. *Atmos. Ocean. Sci. Lett.* **2015**, *5*, 527–533. [[CrossRef](#)]
32. Jiang, D.; Tian, Z.; Lang, X. Reliability of climate models for China through the IPCC Third to Fifth Assessment Reports. *Int. J. Climatol.* **2016**, *36*, 1114–1133. [[CrossRef](#)]
33. Dong, T.-Y.; Dong, W.-J.; Guo, Y.; Chou, J.-M.; Yang, S.-L.; Tian, D.; Yan, D.-D. Future temperature changes over the critical Belt and Road region based on CMIP5 models. *Adv. Clim. Chang. Res.* **2018**. [[CrossRef](#)]
34. Sillmann, J.; Kharin, V.; Zwiers, F.; Zhang, X.; Bronaugh, D. Climate extremes indices in the CMIP5 multimodel ensemble: Part 2. Future climate projections. *J. Geophys. Res. Atmos.* **2013**, *118*, 2473–2493. [[CrossRef](#)]
35. Hu, W.; Zhang, G.; Zeng, G.; Li, Z. Changes in Extreme Low Temperature Events over Northern China under 1.5 °C and 2.0 °C Warmer Future Scenarios. *Atmosphere* **2019**, *10*, 1. [[CrossRef](#)]
36. Thanigachalam, A.; Achutarao, K.M. Extreme Temperatures over India in the 1.5 °C and 2 °C warmer worlds. In Proceedings of the Agu Fall Meeting, New Orleans, LA, USA, 11–15 December 2017.
37. Ruane, A.C.; Phillips, M.M.; Rosenzweig, C. Climate shifts within major agricultural seasons for +1.5 and +2.0 °C worlds: HAPPI projections and AgMIP modeling scenarios. *Agric. For. Meteorol.* **2018**, *259*, 329–344. [[CrossRef](#)]
38. Leng, G. Keeping global warming within 1.5 °C reduces future risk of yield loss in the United States: A probabilistic modeling approach. *Sci. Total Environ.* **2018**, *644*, 52–59. [[CrossRef](#)]
39. Gosling, S.N.; Zaherpour, J.; Mount, N.J.; Hattermann, F.F.; Dankers, R.; Arheimer, B.; Breuer, L.; Ding, J.; Haddeland, I.; Kumar, R. A comparison of changes in river runoff from multiple global and catchment-scale hydrological models under global warming scenarios of 1 °C, 2 °C and 3 °C. *Clim. Chang.* **2017**, *141*, 577–595. [[CrossRef](#)]
40. Schleussner, C.-F.; Lissner, T.K.; Fischer, E.M.; Wohland, J.; Perrette, M.; Golly, A.; Rogelj, J.; Childers, K.; Schewe, J.; Frieler, K. Differential climate impacts for policy-relevant limits to global warming: The case of 1.5 °C and 2 °C. *Earth Syst. Dyn.* **2016**, *7*, 327–351. [[CrossRef](#)]
41. Li, W.; Jiang, Z.; Zhang, X.; Li, L.; Sun, Y. Additional risk in extreme precipitation in China from 1.5 °C to 2.0 °C global warming levels. *Sci. Bull.* **2018**, *63*, 228–234. [[CrossRef](#)]
42. Zhou, M.-Z.; Zhou, G.-S.; Lyu, X.-M.; Zhou, L.; Ji, Y.-H. CMIP5-based threshold-crossing times of 1.5 °C and 2 °C global warming above pre-industrial levels. *Clim. Chang. Res.* **2018**, *14*, 221–227.

43. Karmalkar, A.V.; Bradley, R.S. Consequences of Global Warming of 1.5 °C and 2 °C for Regional Temperature and Precipitation Changes in the Contiguous United States. *PLoS ONE* **2017**, *12*, e0168697. [[CrossRef](#)]
44. Jia, W.; Bo-Tao, Z.; Ying, X. Response of precipitation and its extremes over China to warming: CMIP5 simulation and projection. *Chin. J. Geophys.* **2015**, *58*, 461–473. [[CrossRef](#)]
45. Radinović, D.; Ćurić, M. Criteria for heat and cold wave duration indexes. *Theor. Appl. Climatol.* **2012**, *107*, 505–510. [[CrossRef](#)]
46. Douglas, E.M.; Vogel, R.M.; Kroll, C.N. Trends in floods and low flows in the United States: Impact of spatial correlation. *J. Hydrol.* **2000**, *240*, 90–105. [[CrossRef](#)]
47. Tabari, H.; Marofi, S.; Aeini, A.; Talaee, P.H.; Mohammadi, K. Trend analysis of reference evapotranspiration in the western half of Iran. *Agric. For. Meteorol.* **2011**, *151*, 128–136. [[CrossRef](#)]
48. You, Q.; Min, J.; Kang, S. Rapid warming in the Tibetan Plateau from observations and CMIP5 models in recent decades. *Int. J. Climatol.* **2016**, *36*, 2660–2670. [[CrossRef](#)]
49. Wu, C.; Huang, G.; Yu, H. Prediction of extreme floods based on CMIP5 climate models: A case study in the Beijiang River basin, South China. *Hydrol. Earth Syst. Sci.* **2015**, *19*, 1385–1399. [[CrossRef](#)]
50. Mann, H.B. Nonparametric tests against trend. *Econom. J. Econom. Soc.* **1945**, *13*, 245–259. [[CrossRef](#)]
51. Gocic, M.; Trajkovic, S. Analysis of changes in meteorological variables using Mann-Kendall and Sen's slope estimator statistical tests in Serbia. *Glob. Planet. Chang.* **2013**, *100*, 172–182. [[CrossRef](#)]
52. Sen, P.K. Estimates of the regression coefficient based on Kendall's tau. *J. Am. Stat. Assoc.* **1968**, *63*, 1379–1389. [[CrossRef](#)]
53. Li, D.; Zhou, T.; Zou, L.; Zhang, W.; Zhang, L. Extreme high-temperature events over East Asia in 1.5 °C and 2 °C warmer futures: Analysis of NCAR CESM low-warming experiments. *Geophys. Res. Lett.* **2018**, *45*, 1541–1550. [[CrossRef](#)]
54. Chen, X.; Ying, X.U.; Yao, Y.; Center, H.C.; Center, N.C. Changes in Climate Extremes over China in a 2 °C, 3 °C, and 4 °C Warmer World. *Chin. J. Atmos. Sci.* **2015**, *39*, 1123–1135. [[CrossRef](#)]
55. Yue, S.; Lang, X.; Jiang, D. Projected signals in climate extremes over China associated with a 2 °C global warming under two RCP scenarios. *Int. J. Climatol.* **2018**, *38*, e678–e697.
56. Shuai, J.; Jiang, Z.; Wei, L.; Shen, Y. Evaluation of the Extreme Temperature and Its Trend in China Simulated by CMIP5 Models. *Clim. Chang. Res.* **2017**, *13*, 11–24. [[CrossRef](#)]
57. Jiang, Z.; Song, J.; Li, L.; Chen, W.; Wang, Z.; Wang, J. Extreme climate events in China: IPCC-AR4 model evaluation and projection. *Clim. Chang.* **2012**, *110*, 385–401. [[CrossRef](#)]
58. Dong, S.; Xu, Y.; Zhou, B.; Shi, Y. Assessment of indices of temperature extremes simulated by multiple CMIP5 models over China. *Adv. Atmos. Sci.* **2015**, *32*, 1077–1091. [[CrossRef](#)]
59. Ali, J.; Syed, K.H.; Gabriel, H.F.; Saeed, F.; Ahmad, B.; Bukhari, S.A.A. Centennial Heat Wave Projections Over Pakistan Using Ensemble NEX GDDP Data Set. *Earth Syst. Environ.* **2018**, *2*, 437–454. [[CrossRef](#)]
60. Bao, Y.; Wen, X. Projection of China's near- and long-term climate in a new high-resolution daily downscaled dataset NEX-GDDP. *J. Meteorol. Res.* **2017**, *31*, 236–249. [[CrossRef](#)]
61. Chen, H.-P.; Sun, J.-Q.; Li, H.-X. Future changes in precipitation extremes over China using the NEX-GDDP high-resolution daily downscaled data-set. *Atmos. Ocean. Sci. Lett.* **2017**, *10*, 403–410. [[CrossRef](#)]
62. Perkins-Kirkpatrick, S.E.; Gibson, P.B. Changes in regional heatwave characteristics as a function of increasing global temperature. *Sci. Rep.* **2017**, *7*, 12256. [[CrossRef](#)]
63. Zhan, M.; Xiucang, L.I.; Sun, H.; Zhai, J.; Jiang, T.; Wang, Y. Changes in Extreme Maximum Temperature Events and Population Exposure in China under Global Warming Scenarios of 1.5 and 2.0 °C: Analysis Using the Regional Climate Model COSMO-CLM. *J. Meteorol. Res.* **2018**, *32*, 99–112. [[CrossRef](#)]

